NASA TN D-921

TECHNICAL NOTE

D-921

EXPERIMENTAL INVESTIGATION AT MACH NUMBER 3.0 OF THE EFFECTS OF THERMAL STRESS AND BUCKLING ON THE FLUTTER OF FOUR-BAY ALUMINUM ALLOY PANELS WITH LENGTH-WIDTH RATIOS OF 10

By Sidney C. Dixon, George E. Griffith,
and Herman L. Bohon

Langley Research Center
Langley Field, Va.

NATIONAL AERONAUTICS AND SPACE ADMINISTRATION
WASHINGTON October 1961

NATIONAL AERONAUTICS AND SPACE ADMINISTRATION

TECHNICAL NOTE D-921

EXPERIMENTAL INVESTIGATION AT MACH NUMBER 3.0 OF THE EFFECTS OF THERMAL STRESS AND BUCKLING ON THE FLUTTER OF FOUR-BAY ALUMINUM ALLOY PANELS WITH LENGTH-WIDTH RATIOS OF 10

By Sidney C. Dixon, George E. Griffith,
and Herman L. Bohon

SUMMARY

Skin-stiffener aluminum alloy panels consisting of four bays, each bay having a length-width ratio of 10, were tested at a Mach number of 3.0 at dynamic pressures ranging from 1,500 psf to 5,000 psf and at stagnation temperatures from 300° F to 655° F. The panels were restrained by the supporting structure in such a manner that partial thermal expansion of the skins could occur in both the longitudinal and lateral directions.

A boundary faired through the experimental flutter points consisted of a flat-panel portion, a buckled-panel portion, and a transition point at the intersection of the two boundaries. In the region where a panel must be flat when flutter occurs, an increase in panel skin temperature (or midplane compressive stress) makes the panel more susceptible to flutter. In the region where a panel must be buckled when flutter occurs, the flutter trend is reversed. This reversal in trend is attributed to the panel postbuckling behavior.

INTRODUCTION

The problem of panel flutter has currently become acute since panel flutter has been encountered by aircraft operating at supersonic speeds. Moreover, aerodynamic heating associated with supersonic flight and the resulting compressive stresses can alter panel stiffness and consequently play an important role in panel flutter. Very little is known theoretically about the flutter behavior of panels acted upon by compressive forces, even in the nonbuckled range, and no theoretical information seems to exist on the effects of post-buckling behavior on the flutter characteristics of finite panels.

The effects of midplane compressive stress have been investigated experimentally through mechanical buckling (with some heating) of simple, clamped plates having length-width ratios of 5 or less. (See, for example, refs. 1 to 4.) In addition, some initial results of an exploratory investigation of the effects of aerodynamic heating on multibay panels with length-width ratios of 10 were presented in a summary paper on panel flutter (ref. 5). These results showed that compressive stresses induced by aerodynamic heating could initiate flutter of a flat panel that would otherwise be stable and, also, that additional heating could stop the flutter; this latter phenomenon was attributed to the post-buckling behavior of the panels.

The present investigation, conducted in the Langley 9- by 6-foot thermal structures tunnel, was undertaken to study in more detail the effects of compressive stress and buckling (induced by aerodynamic heating) on panel flutter and to provide additional experimental flutter data for panels with length-width ratios of 10. Aluminum alloy panels consisting of four bays, each bay having a length-width ratio of 10, were tested at a Mach number of 3.0 at various dynamic pressures and stagnation temperatures. Panel skin thicknesses were 0.025, 0.032, and 0.040 inch. The panels were restrained by the supporting structure so that partial thermal expansion of the skin could occur in both the longitudinal and lateral directions. The differential pressure acting on the panels was kept small in order to eliminate the differential pressure from the variables in the program.

The flutter data obtained in this investigation are presented in tabular form and are also summarized in terms of nondimensional parameters in the form of a flutter boundary to indicate the overall effects of midplane compressive stresses and buckling on panel flutter.

SYMBOLS

a	length, parallel to airflow (see fig. 4)
b	width, perpendicular to airflow (see fig. 4)
C_p	pressure coefficient, $\frac{p - p_\infty}{q}$
c	specific heat of panel material
D	panel flexural rigidity, $\frac{E\tau^3}{12(1 - \mu^2)}$
E	Young's modulus

f	frequency of flutter
h	aerodynamic heat-transfer coefficient
l	panel length (longitudinal direction, parallel to airflow)
M	Mach number
p	static pressure
p_b	static pressure in bay behind panel
p_∞	free-stream static pressure
Δp	differential pressure acting on panel skin, $p_b - p_\infty$
q	dynamic pressure
T	temperature
T_{aw}	adiabatic-wall temperature
T_i	initial temperature of panel
T_t	stagnation temperature
T_∞	free-stream temperature
ΔT	average increase of panel skin temperature (along center line of bays)
t	time
t_i	time at which panel becomes exposed to airflow
w	bay width (lateral direction, perpendicular to airflow)
x,y	Cartesian coordinates (see fig. 4)
α	coefficient of thermal expansion
η_r	recovery factor, $\frac{T_{aw} - T_\infty}{T_t - T_\infty}$
μ	Poisson's ratio
ρ	specific weight of panel material

σ midplane stress in direction of airflow

τ panel skin thickness

TESTS

Panels

The panels were of skin-stiffener construction and had four bays, each 26 inches long and 2.60 inches wide. The panel skins consisted of flat sheets of 0.025-, 0.032-, or 0.040-inch-thick 2024-T3 aluminum alloy riveted to five longitudinal channel-section stiffeners and two lateral Z-section stiffeners. The stiffeners were approximately 1.5 inches deep and were formed from 0.051-inch-thick 2024-T3 aluminum alloy. Four steel channels were riveted across the bottom of the stiffeners to provide support for mounting instrumentation. A rear-view photograph of a typical panel is shown in figure 1, and pertinent panel construction details are given in figure 2.

L 1 2 6 5

Test Apparatus

Langley 9- by 6-foot thermal structures tunnel.- All tests were conducted in the Langley 9- by 6-foot thermal structures tunnel, an intermittent blowdown facility operating at a Mach number of 3.0 and exhausting to the atmosphere. A heat exchanger is preheated to provide stagnation temperatures up to 660° F. During tunnel starting and shutdown, the flow separates from the nozzle walls with the result that unprotected specimens are buffeted by very turbulent air and are subjected to loads considerably in excess of those applied during the period of test conditions. (See the appendix for additional details regarding the tunnel.)

Panel holder and mounting arrangement.- The panels were mounted in a panel holder which extended vertically through the test section (fig. 3). The panel holder has a beveled half-wedge leading edge, flat sides, and a recess 29 inches wide and 30 inches high for accommodating test specimens. The recess is located on the nonbeveled side of the panel holder. Pneumatically operated sliding doors protect test specimens from aerodynamic buffeting and heating during tunnel starting and shutdown. Aerodynamic fences prevent shock waves emanating from the doors from interfering with the airflow over the test specimen. A vent-door arrangement on the side opposite the panel recess is used to control the pressure inside the chamber behind the test specimen. The flow conditions over the area of the recess, determined from pressure

surveys of a flat calibration panel (29 inches by 30 inches), are indicated in figure 4 in terms of the pressure coefficient C_p. As can be seen from figure 4, the flow conditions were essentially free-stream conditions.

All panels were mounted so as to form a section of the flat surface of the panel holder (fig. 3). The panels were attached to 0.375-inch-thick steel filler plates by means of 0.125-inch-thick steel angles to provide support along the longitudinal edges as shown in figure 5(a); figure 5(b) shows the manner in which the panels were supported at the leading and trailing edges. This mounting arrangement allowed partial thermal expansion of the panel skin in the longitudinal and lateral directions.

Instrumentation

Iron-constantan thermocouples, spotwelded to the panels at the 12 locations shown in figure 6, were used to measure panel temperatures. Inductance-type deflectometers were used to determine panel skin deflections. The deflectometers were located approximately one-quarter inch behind the panel skin at the 6 positions indicated in figure 6. In addition, high-speed 16-millimeter motion pictures taken at speeds up to 2,660 frames per second provided supplementary data on panel behavior. The panel skins were painted to form grid lines for photographic purposes.

Quick-response, strain-gage-type pressure transducers were used to measure tunnel static pressures and the static pressures at various locations on the panel holder and in the chamber behind the panels. Tunnel stagnation pressures were obtained from static pressures measured in the settling chamber. Stagnation temperatures were measured by total-temperature probes located in the test section. For each test all temperature and pressure data, for both the test panels and the tunnel operating conditions, were recorded on magnetic tape. Deflection data were recorded on high-speed oscillographs.

Test Procedure

All tests were conducted at a Mach number of 3.0, at dynamic pressures ranging from 1,500 psf to 5,000 psf, and at stagnation temperatures from 300° F to 655° F. The protective doors on the panel holder were opened only after desired test conditions were established. The dynamic pressure was maintained constant during the first portion of all tests but generally was varied near the end of the tests. The usual procedure for varying the dynamic pressure was as follows: (a) if

no flutter had occurred near the end of a test, the dynamic pressure was increased in an attempt to initiate flutter; (b) if flutter had started and stopped, the dynamic pressure was increased in an attempt to restart flutter; or (c) if the panel was fluttering near the end of a test, the dynamic pressure was decreased in an attempt to stop flutter. The differential pressure on the panels was kept small (usually less than 70 psf) in order to eliminate the differential pressure from the variables in the program. The stagnation temperature was essentially constant during a test. The protective doors were closed 3 seconds prior to tunnel shutdown. The duration of test conditions was approximately 20 to 30 seconds.

RESULTS AND DISCUSSION

In 18 of the 20 tests made in this investigation flutter was induced in panels that were flat prior to the start of flutter; in 16 of these tests the dynamic pressure was constant when flutter occurred but was increasing in the other 2 tests. The flutter stopped in 8 of these tests; at the cessation of flutter the panels were in a buckled condition. The dynamic pressure was constant in 4 tests when flutter stopped and was decreasing for the other 4 tests. In 2 tests, after flutter stopped - as noted, the panels were then buckled - flutter was restarted by increasing the dynamic pressure. No flutter occurred in 2 tests. Pertinent data for all tests are given in table I. The data tabulated are the dynamic pressure q, panel differential pressure Δp, stagnation temperature T_t, average panel-skin center-line temperature T, the average skin temperature increase ΔT, and the frequency at the start of flutter f.

Panel Temperatures

At the beginning of a test the panel skin and supporting structure were essentially at the same temperature. Any temperature increase of the panels prior to opening the panel-holder protective doors was usually insignificant. After the panels were exposed to the airstream, the skin temperature increased in a manner similar to the typical temperature histories shown in figure 7. This figure shows the measured panel temperatures for test 5. The top curve represents the average skin temperature measured at the center line of the bays. As the average value agreed within 5° F of the individual temperatures, the longitudinal temperature variation was considered insignificant. The temperature histories for thermocouples 1, 6, 8, 9, and 10 indicate that there were appreciable lateral temperature gradients in the skin and large temperature gradients in the supporting structure. However,

these temperature variations were neglected in analyzing the test data because of the lack of sufficient temperature data for some of the panels. For several panels all or most of the skin thermocouples were lost during testing. Hence, for these panels calculated center-line temperatures were used. Calculated temperatures were obtained from the following equation (given in ref. 6):

$$T = T_{aw} - (T_{aw} - T_i)e^{\frac{-h(t-t_i)}{c\rho\tau}} \tag{1}$$

which neglects temperature variation through the skin, heat flow by conduction, and heat transfer by radiation. The aerodynamic heat-transfer coefficients were obtained from the turbulent flow, flat-plate theory presented in reference 7 by using initial free-stream flow conditions and a skin temperature equal to T_i. Temperature calculations based on adiabatic-wall temperatures obtained in the usual manner $\left((T_{aw})_{calc} = \eta_r(T_t - T_\infty) + T_\infty\right.$, where η_r is the turbulent flow recovery factor$\left.\right)$ gave skin temperatures appreciably higher than the measured temperatures. Detailed temperature-distribution calculations which included the effects of heat conduction to the supporting structure indicated that approximately one-third of the difference in measured and calculated temperatures could be accounted for by conduction effects; the remainder of the difference, however, could not be explained. An arbitrary adjustment of the adiabatic-wall temperature was made by using the relation

$$(T_{aw})_{adj} = 0.75(T_{aw})_{calc} \tag{2}$$

Use of this entirely empirical relationship in equation (1) resulted in fairly good agreement between measured and calculated center-line temperatures for all tests where measured temperatures were available. Figure 7 shows a comparison of measured and calculated temperatures for a typical test (test 5).

Flutter Results

Flutter parameters.- The flutter data obtained in this investigation are presented in terms of a nondimensional flutter parameter $\left(\sqrt{M^2 - 1}\,\frac{E}{q}\right)^{1/3}\frac{\tau}{l}$ and a nondimensional temperature parameter $\frac{\alpha\,\Delta T_w^2}{\tau^2}$.

Of the quantities in the flutter parameter $\left(\sqrt{M^2 - 1}\,\frac{E}{q}\right)^{1/3}\frac{\tau}{l}$, which is

the primary panel flutter parameter given by theory, only the dynamic pressure q and skin thickness τ were varied in this investigation. Due to the short duration of the tests, changes in material properties with temperature were assumed negligible.

The second parameter is a measure of the midplane compressive stress in the skin in terms of the temperature rise and is proportional to the ratio of midplane stress to Euler's buckling stress $\frac{\sigma_{\tau w}^2}{\pi^2 D}$. The temperature parameter $\frac{\alpha \Delta T_w^2}{\tau^2}$ neglects the reduction in stress due to thermal expansion and flexibility of the supporting structure. However, since both the supporting structure and edge restraints were essentially identical for all panels, neglect of the supporting structure flexibility should not appreciably affect the nature of the results. In addition, in most tests the temperature change of the supporting structure was insignificant at the start of flutter, which usually occurred within 3 seconds after the panels were exposed to the airstream. Although the temperature increased appreciably thereafter (see, for example, fig. 7), the overall restraint of the mounting fixture was such as to minimize the thermal expansion of the supporting structure. Thus, the temperature parameter $\frac{\alpha \Delta T_w^2}{\tau^2}$ was adjudged adequate to show the experimental flutter trends. This parameter also neglects the effects of nonuniform midplane stress in the skin, but variations in the estimated stress distribution were considered insufficient to affect the flutter trends.

L 1 2 6 5

Neither the flutter parameter nor the temperature parameter accounts for the effects of differential pressure. However, the differential pressures were relatively small (usually less than 70 psf), so that the overall effect on the results was considered insignificant.

Effect of compressive stress and buckling on flutter.- The effects of compressive stress and buckling can be seen from the results of a typical test where flutter started, stopped, and restarted, as shown in figure 8 in terms of the flutter parameter and the temperature parameter. The dashed line in figure 8 represents the variation in the parameters due to changes in the dynamic pressure and panel skin temperature during the test. In this test (test 16), the dynamic pressure was constant for the first 17 seconds $\left(\text{up to } \frac{\alpha \Delta T_w^2}{\tau^2} = 16.7\right)$ as indicated by the horizontal portion of the dashed line; thus the only significant variable during this part of the test was the panel skin temperature. The panel remained in a stable, flat condition until the skin temperature reached 235° F; at this point the panel became unstable and began to

flutter, as indicated by the open symbol in figure 8. Flutter continued for about 8 seconds under constant dynamic pressure until the skin temperature reached 374° F at which point flutter stopped, as indicated by the solid symbol. The panel was observed to be in a buckled state immediately following the cessation of flutter. In order to induce flutter of the stable, buckled panel it was necessary to increase the dynamic pressure as indicated by the drop in the flutter parameter in figure 8. After an appreciable increase in dynamic pressure (from 3,485 psf to 4,880 psf) the panel became unstable and fluttered to the end of the test as shown by the open symbol with the tick mark.

L
1
2
6
5

The results of all tests are presented in figure 9 in terms of the flutter parameter and the differential temperature parameter to show the overall effects of compressive stress and buckling on panel flutter. Again, the open symbols represent flutter start points where the panels were flat prior to the start of flutter, the solid symbols represent flutter stop points (panel buckled), and the open symbols with tick marks are flutter start points for panels that were buckled prior to flutter. The half-solid symbols represent no-flutter points. The solid curve is a boundary faired through the experimental flutter points.

As can be seen from figure 9, the flutter boundary consists of a flat panel portion, a buckled panel portion, and a transition point at the intersection of the two boundaries. To the left of the transition point $\left(\frac{\alpha\ \Delta T_w^2}{\tau^2} < 12\right)$ a panel must be flat if flutter is to occur. For a given panel and aerodynamic conditions, an increase in panel skin temperature (an indication of thermal stress) will make a flat panel more susceptible to flutter as indicated by the flutter trend of the flat panel boundary. To the right of the transition point $\left(\frac{\alpha\ \Delta T_w^2}{\tau^2} > 12\right)$ the flutter trend is reversed. This reversal in trend is attributed to the panel postbuckling behavior; once a panel becomes thermally buckled, any additional temperature rise will tend to stiffen the panel (by increasing the depth of buckle) as shown both theoretically and experimentally in references 8 and 9. Thus, to the right of the transition point, where a stable panel must be buckled, an increase in temperature will make a panel less susceptible to flutter. As can be seen from figure 9, within the scatter of the data, the points representing flutter start (panel buckled) agree with the boundary established by the flutter stop points. Thus, when this boundary is crossed from above, a buckled panel becomes unstable and flutters, or when crossed from below, flutter stops and the panel becomes stable but buckled.

At the transition point, the skin thickness required to prevent flutter for a given dynamic pressure is a maximum and is approximately three times the thickness required to prevent flutter of an unheated

panel. Thus, it appears that the effects of thermal stress (induced by aerodynamic heating) on panel flutter are of sufficient magnitude to make mandatory the consideration of these effects in the design of supersonic aircraft.

Flutter Behavior

High-speed motion pictures revealed that all observed flutter was of the sinusoidal traveling-wave type. The flutter mode had approximately eight waves in the longitudinal direction and appeared to be similar to the buckling mode shape. Although most observed flutter was relatively mild, one panel with a skin thickness of 0.025 inch was damaged (test 1); figure 10 shows this damage which occurred near the trailing edge of the panel. Flutter began at a dynamic pressure of 3,270 psf and the damage occurred approximately 17.5 seconds later when the dynamic pressure had reached 4,470 psf and the skin temperature 322° F.

L 1 2 6 5

For tests in which flutter was induced in a flat panel, the flutter amplitude always increased gradually to a maximum (fig. 11(a)) and then usually remained constant (fig. 11(b)). When the maximum amplitude did not remain constant, two types of variable amplitude flutter were observed. The first of these, similar to the phenomenon known as beating - where the amplitude varies in a relatively uniform fashion, is illustrated in figure 11(c). The second type, shown in figure 11(d), is an irregular amplitude flutter which sometimes occurred after flutter had been sustained for several seconds.

For tests wherein flutter occurred after the panel had been thermally buckled, flutter started more abruptly. However, a short burst of random, very low frequency oscillation preceded the start of flutter, as can be seen in figure 11(e). Immediately prior to the cessation of flutter, there usually was a large reduction in frequency and the motion rapidly changed to a very low frequency oscillation which became intermittent and stopped, as shown in figure 11(f). Although the intermittent motion did not occur in all bays of a given panel for the same duration of time, all bays essentially started or stopped fluttering in unison.

CONCLUSIONS

Skin-stiffener aluminum-alloy panels consisting of four bays, each bay having a length-width ratio of 10, were tested in the Langley 9- by 6-foot thermal structures tunnel (a blowdown facility) to determine

the effects of thermal stress and buckling on panel flutter. The tests were conducted at a Mach number of 3.0 at dynamic pressures ranging from 1,500 psf to 5,000 psf and at stagnation temperatures from 300° F to 655° F. The panel supporting structure restrained the panels in such a manner that partial thermal expansion of the skins could occur in both the longitudinal and lateral directions. The tests revealed the following:

1. An overall flutter boundary, faired through the experimental points, consists of a flat panel portion, a buckled panel portion, and a transition point at the intersection of the two.

2. The flat panel boundary reveals that, for a given panel and aerodynamic conditions, an increase in panel skin temperature (or mid-plane compressive stress) makes a flat panel more susceptible to flutter.

3. For the buckled panel boundary the flutter trend is reversed; this reversal in trend is attributed to the panel postbuckling behavior. Once a panel becomes thermally buckled, any additional temperature rise tends to stiffen the panel by increasing the depth of buckle.

4. At the transition point, the skin thickness required to prevent flutter is a maximum and is approximately three times the thickness required to prevent flutter of an unheated panel.

Langley Research Center,
National Aeronautics and Space Administration,
Langley Field, Va., May 11, 1961.

APPENDIX

LANGLEY 9- BY 6-FOOT THERMAL STRUCTURES TUNNEL

The Langley 9- by 6-foot thermal structures tunnel is an intermittent blowdown supersonic wind tunnel exhausting to the atmosphere through a diffuser. Figure 12 shows a cross section of the tunnel along the longitudinal center line of the nozzle.

Air is released from a bottle storage field by quick-acting rotor valves automatically regulated to provide preset stagnation pressures up to 200 psia. The stagnation pressure may be varied during a test but only by manual valve control. When the valves are opened, the air passes into a heat exchanger which is preheated to provide stagnation temperatures up to 660° F. The air then passes through a nozzle (designed for a Mach number of 3.0) into the test section.

The test section is 6 feet high, 8 feet 9 inches wide, and 10 feet long. Test specimens may be mounted on a turntable, the top of which is flush with the floor of the test section. Ports in the top and side walls of the test section provide windows for lighting and motion-picture and television cameras. Operation of the tunnel and the sequence of events for a test is controlled by an automatic programer.

Quick response, strain-gage-type pressure transducers are used to measure tunnel static pressures. Tunnel stagnation pressures are obtained from static pressures measured in the settling chamber. Stagnation temperatures are measured by total temperature probes located in the test section. Data for both the tunnel and models can be recorded on oscillographs or on magnetic tape.

Performance characteristics for the tunnel are:

Stagnation pressure, psia	55 to 200
Dynamic pressure, psf	1,400 to 5,000
Stagnation temperature, °F	200 to 660
Approximate time to start, sec	1
Approximate time to shutdown, sec	5
Running time, sec	Up to 55

During tunnel starting and shutdown, the flow separates from the nozzle walls with the result that unprotected test specimens are buffeted by very turbulent air and are subjected to loads considerably in excess of those applied during the period of test conditions.

REFERENCES

1. Sylvester, Maurice A., and Baker, John E.: Some Experimental Studies of Panel Flutter at Mach Number 1.3. NACA TN 3914, 1957. (Supersedes NACA RM L52I16.)

2. Sylvester, Maurice A., Nelson, Herbert C., and Cunningham, Herbert J.: Experimental and Theoretical Studies of Panel Flutter at Mach Numbers 1.2 to 3.0. NACA RM L55E18b, 1955.

3. Sylvester, Maurice A.: Experimental Studies of Flutter of Buckled Rectangular Panels at Mach Numbers From 1.2 to 3.0 Including Effects of Pressure Differential and of Panel Width-Length Ratio. NASA TN D-833, 1961. (Supersedes NACA RM L55I30.)

4. Eisley, Joe Griffin: Panel Flutter in Supersonic Flow. Ph.D. Thesis, C.I.T., 1956.

5. Kordes, Eldon E., Tuovila, Weimer J., and Guy, Lawrence D.: Flutter Research on Skin Panels. NASA TN D-451, 1960.

6. Heldenfels, Richard R., Rosecrans, Richard, and Griffith, George E.: Test of an Aerodynamically Heated Multiweb Wing Structure (MW-1) in a Free Jet at Mach Number 2. NACA RM L53E27, 1953.

7. Lee, Dorothy B., and Faget, Maxime A.: Charts Adapted From Van Driest's Turbulent Flat-Plate Theory for Determining Values of Turbulent Aerodynamic Friction and Heat-Transfer Coefficients. NACA TN 3811, 1956.

8. Bisplinghoff, R. L., and Pian, T. H. H.: On the Vibrations of Thermally Buckled Bars and Plates. Tech. Rep. 25-22, Office of Naval Res., Sept. 1956.

9. Shulman, Yechiel: On the Vibration of Thermally Stressed Plates in the Pre-Buckling and Post-Buckling States. Tech. Rep. 25-25, Office of Naval Res., Jan. 1958.

TABLE I.- PANEL FLUTTER DATA

$$\left[E = 10.5 \times 10^6 \text{ psi}; \ \alpha = 12.6 \times 10^{-6} \ \frac{\text{in./in.}}{^\circ F}\right]$$

Test	τ, in.	T_t, $^\circ F$	Flutter start					Flutter stop				No flutter			
			q, psf	Δp, psf	T, $^\circ F$	ΔT, $^\circ F$	f, cps	q, psf	Δp, psf	T, $^\circ F$	ΔT, $^\circ F$	q, psf	Δp, psf	T, $^\circ F$	ΔT, $^\circ F$
1	0.025	500	3,270	63	102	39	685								
2	.025	650	3,270	63	110	56	650								
3	.025	445	2,530	-46	122	40	655								
4	.025	300	4,950	-33	109	23	760								
5	.032	405	3,280	-22	148	93	705								
6	.032	655	3,280	13	139	83	712								
7	.032	410	4,020	-24	139	72	798								
8	.032	640	2,280	-63	151	81	705	2,280	52	262	192				
9	.032	485										1,510	56	215	133
10	.032	650	2,750	101	123	86	670	2,750	72	219	144				
11	.040	330										4,410	-19	201	123
12	.040	650	4,560	-22	213	155	760	[c]3,960	-22	343	285				
13	.040	510	3,270	-23	263	191	717								
14	.040	650	3,220	56	205	142	720	3,220	32	338	275				
15	.040	550	3,280	45	215	137	730								
16	.040	650	3,510	66	235	161	825	[c]3,485	68	374	300				
			[a] [b]4,880	59	401	327	550								
17	.040	540	2,755	-69	271	195	720								
18	.040	590	2,520	37	319	239	615	2,520	40	335	255				
			[a] [b]4,350	53	377	297	495								
19	.040	550	[b]3,840	48	308	223	690	[c]4,300	89	374	289				
20	.040	545	[b]2,530	53	298	225	690	[c]2,780	83	333	260				

[a]Panel buckled prior to start of flutter.
[b]Dynamic pressure increasing.
[c]Dynamic pressure decreasing.

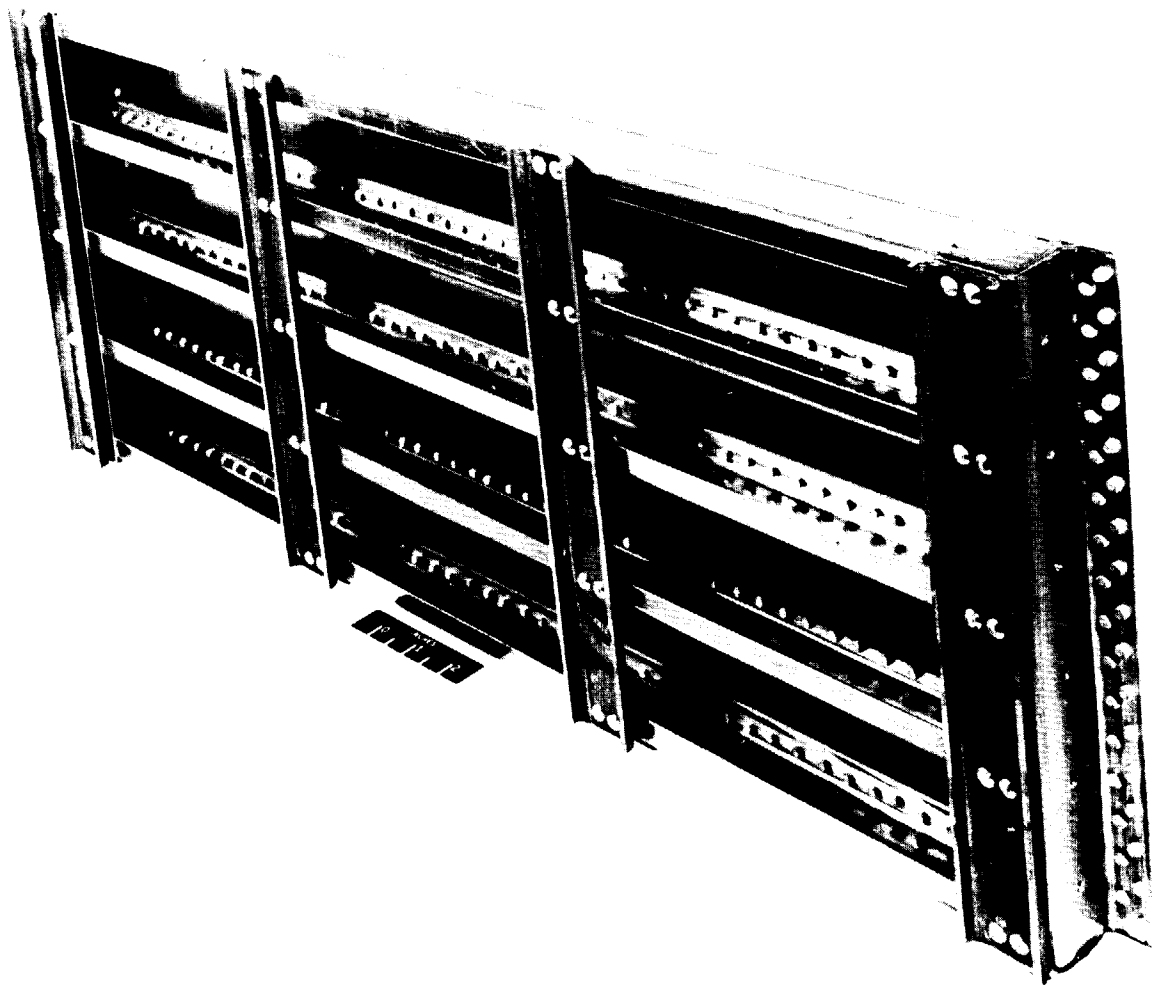

Figure 1.- Rear view of typical panel. L-60-2686

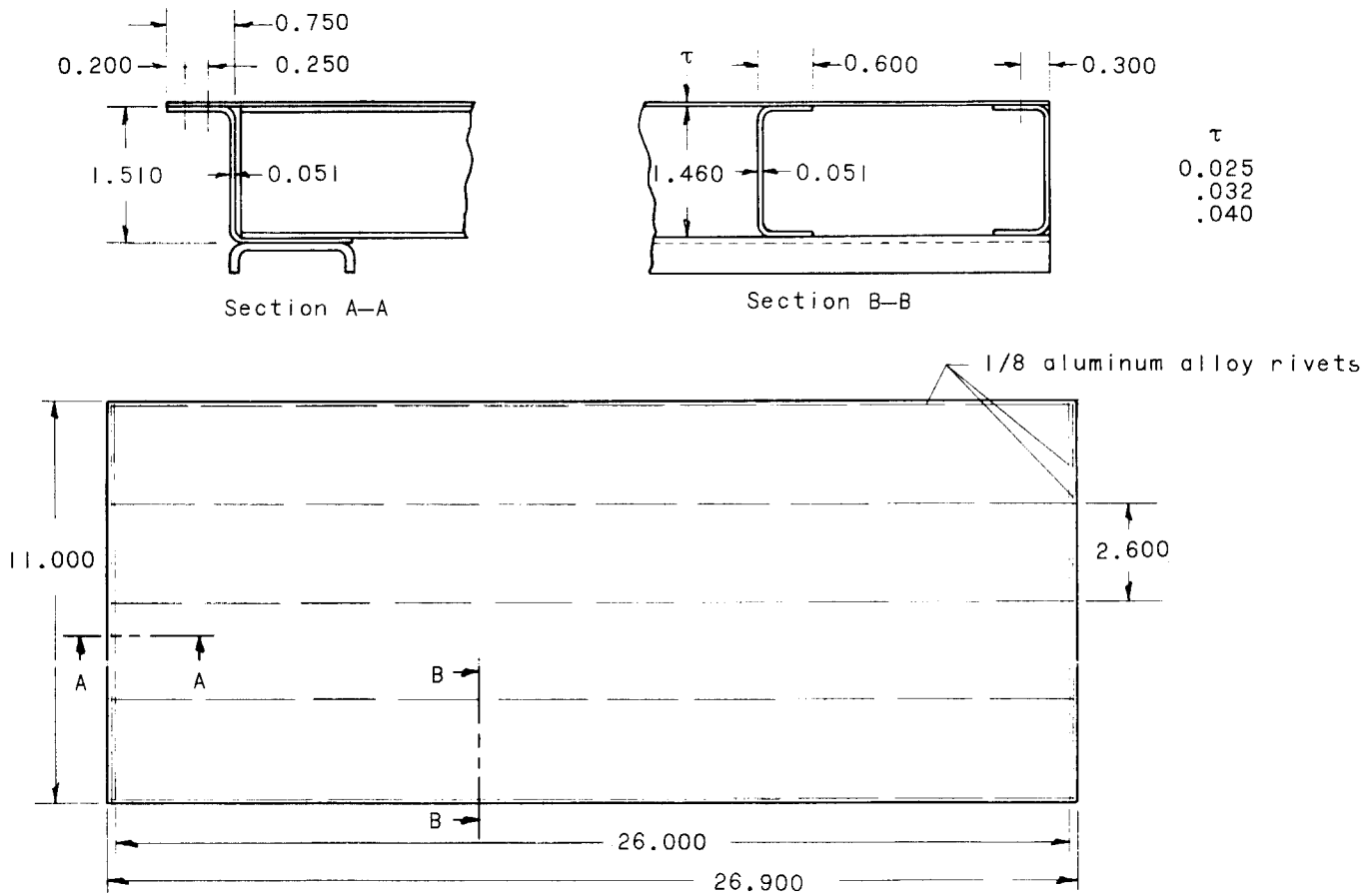

Figure 2.- Panel construction details. Typical for all panels. All dimensions are in inches.

L-1265

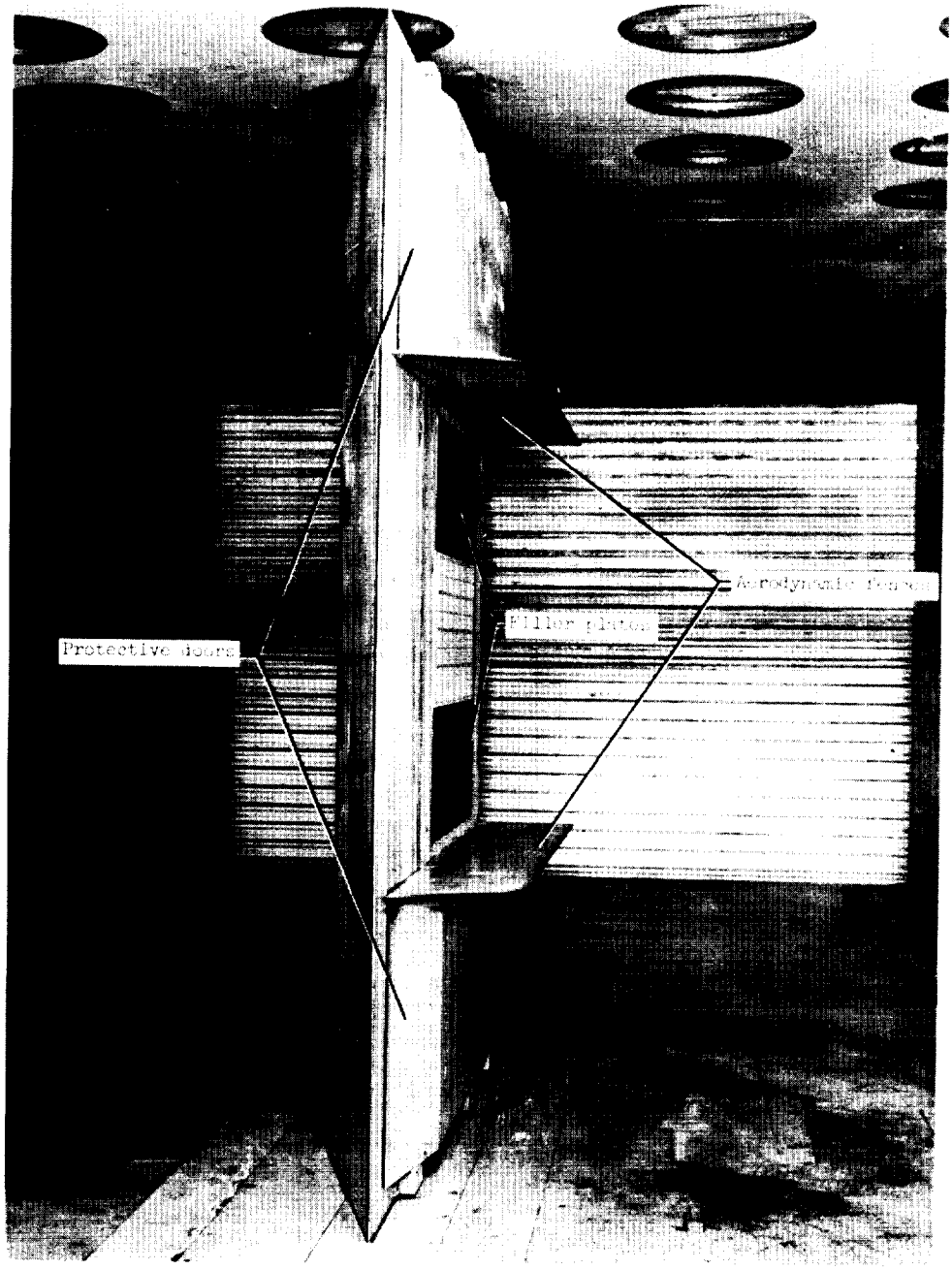

L-60-1859.1

Figure 3.- Panel mounted in panel holder in test section as viewed from upstream. Panel holder protective doors are in open position. Tunnel exit door is closed.

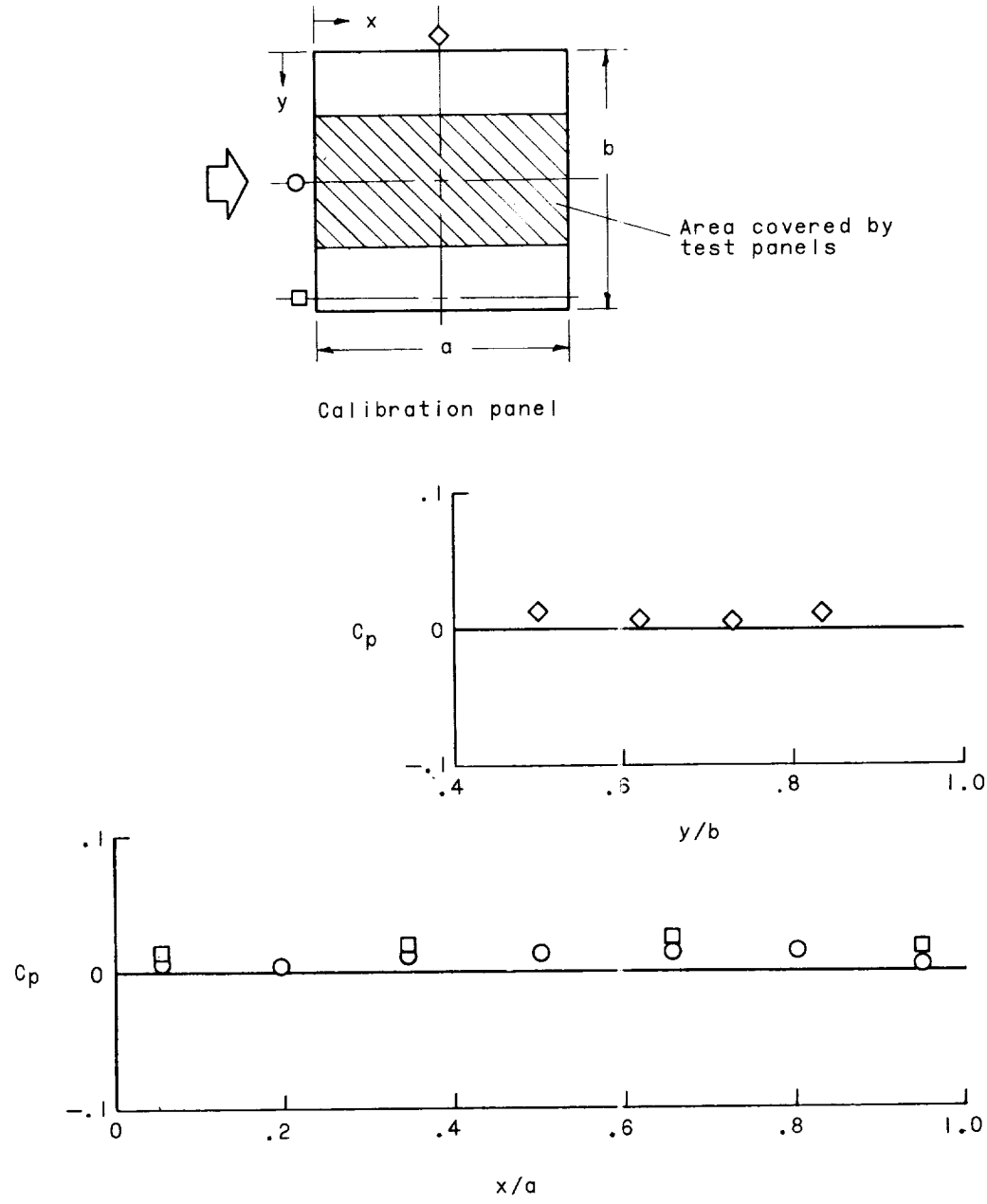

Figure 4.- Pressure distribution over a flat plate mounted in panel holder.

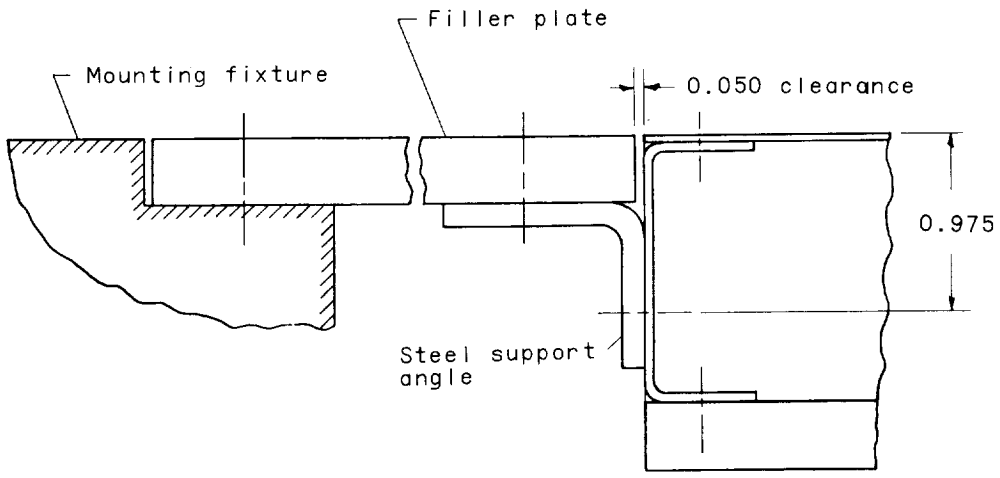

(a) Longitudinal edges.

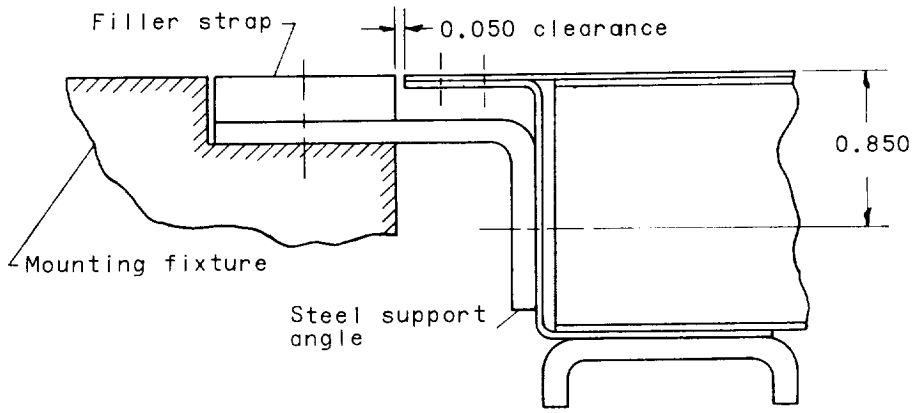

(b) Leading and trailing edges.

Figure 5.- Panel mounting arrangements. Typical for all panels.

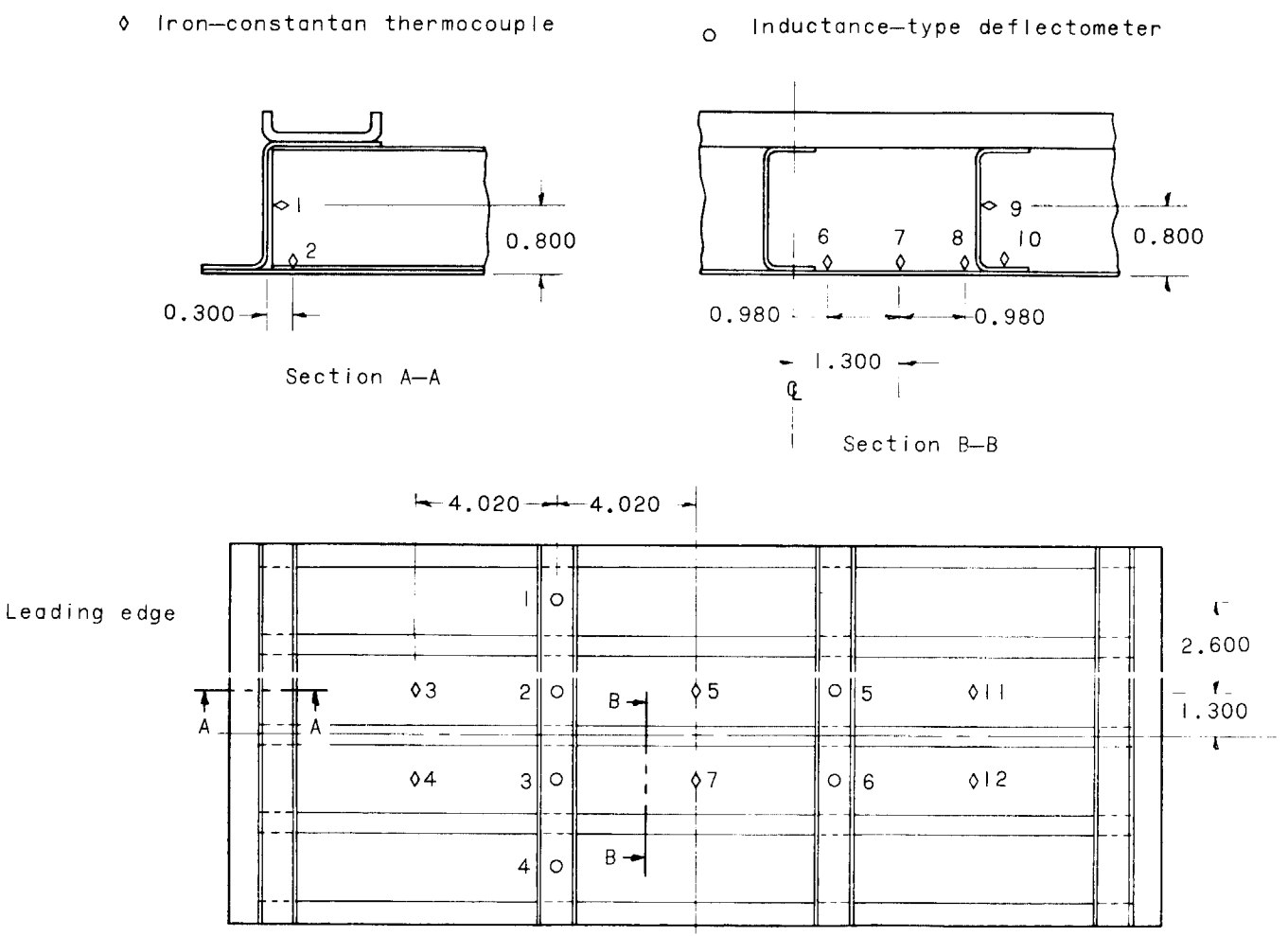

Figure 6.- Location of panel instrumentation. All dimensions are in inches.

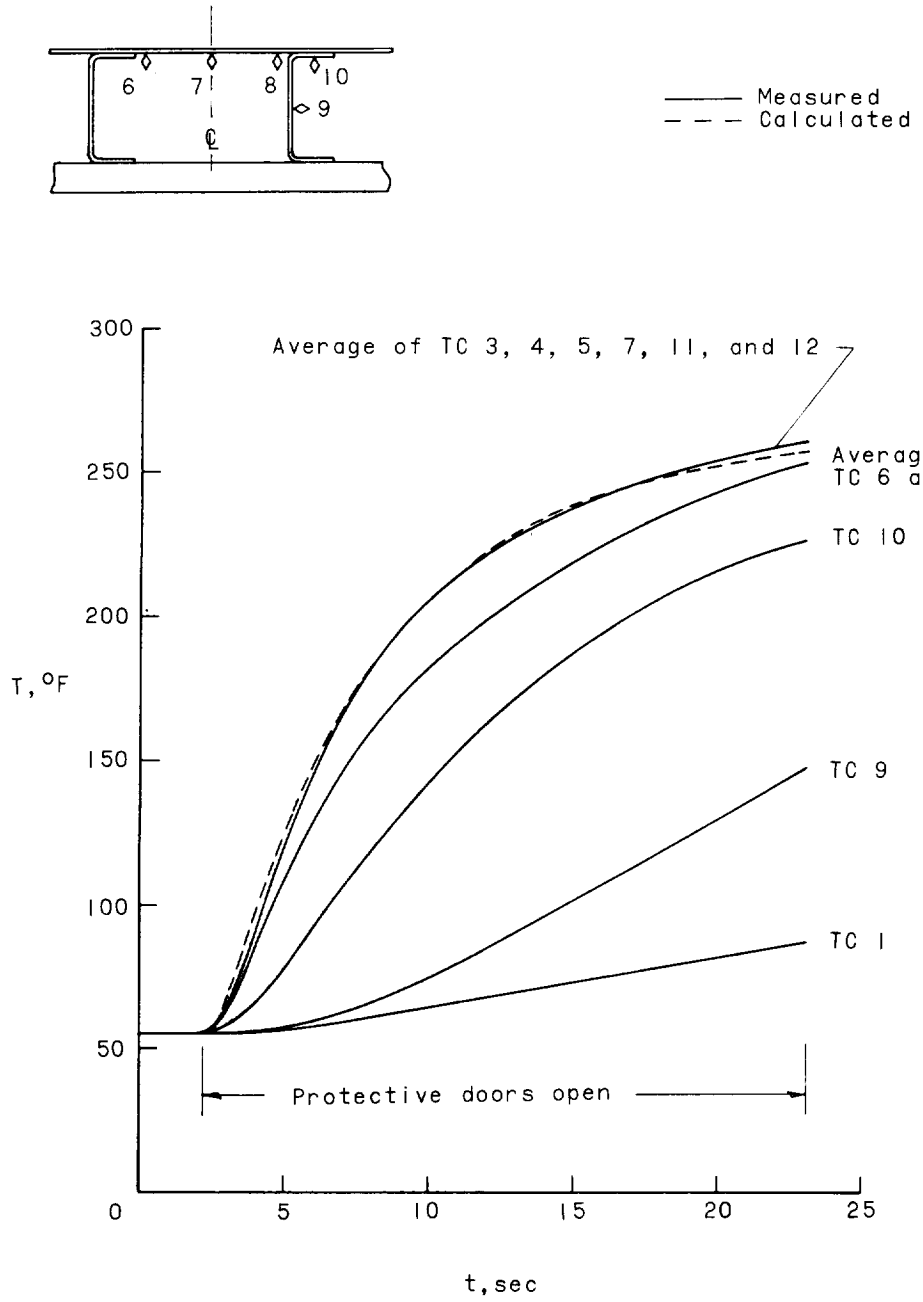

L-1265

Figure 7.- Measured and calculated panel temperatures for test 5.

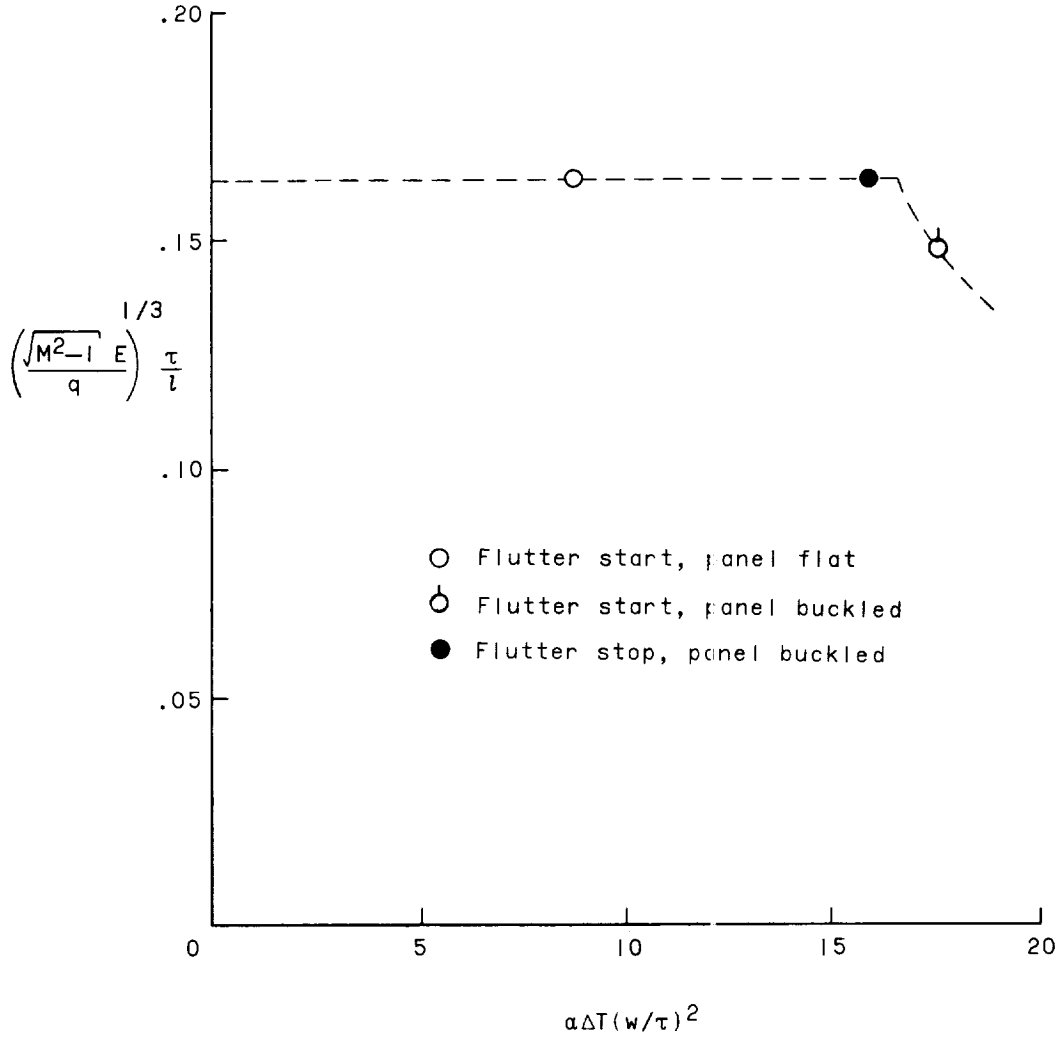

L-1265

Figure 8.- Variation of flutter parameters during test in which flutter started, stopped, and restarted.

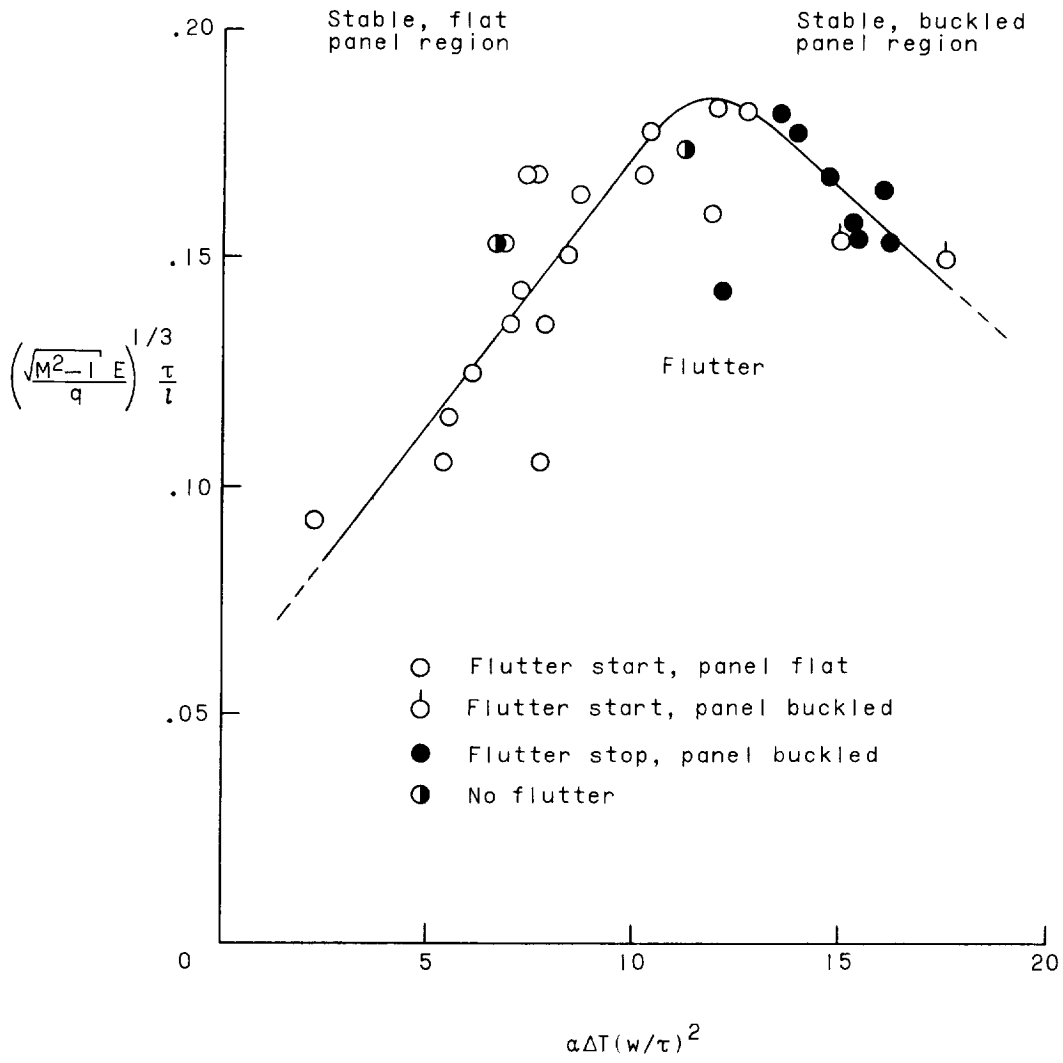

Figure 9.- Effects of aerodynamic heating on flutter of partially restrained panels with length-width ratios of 10.

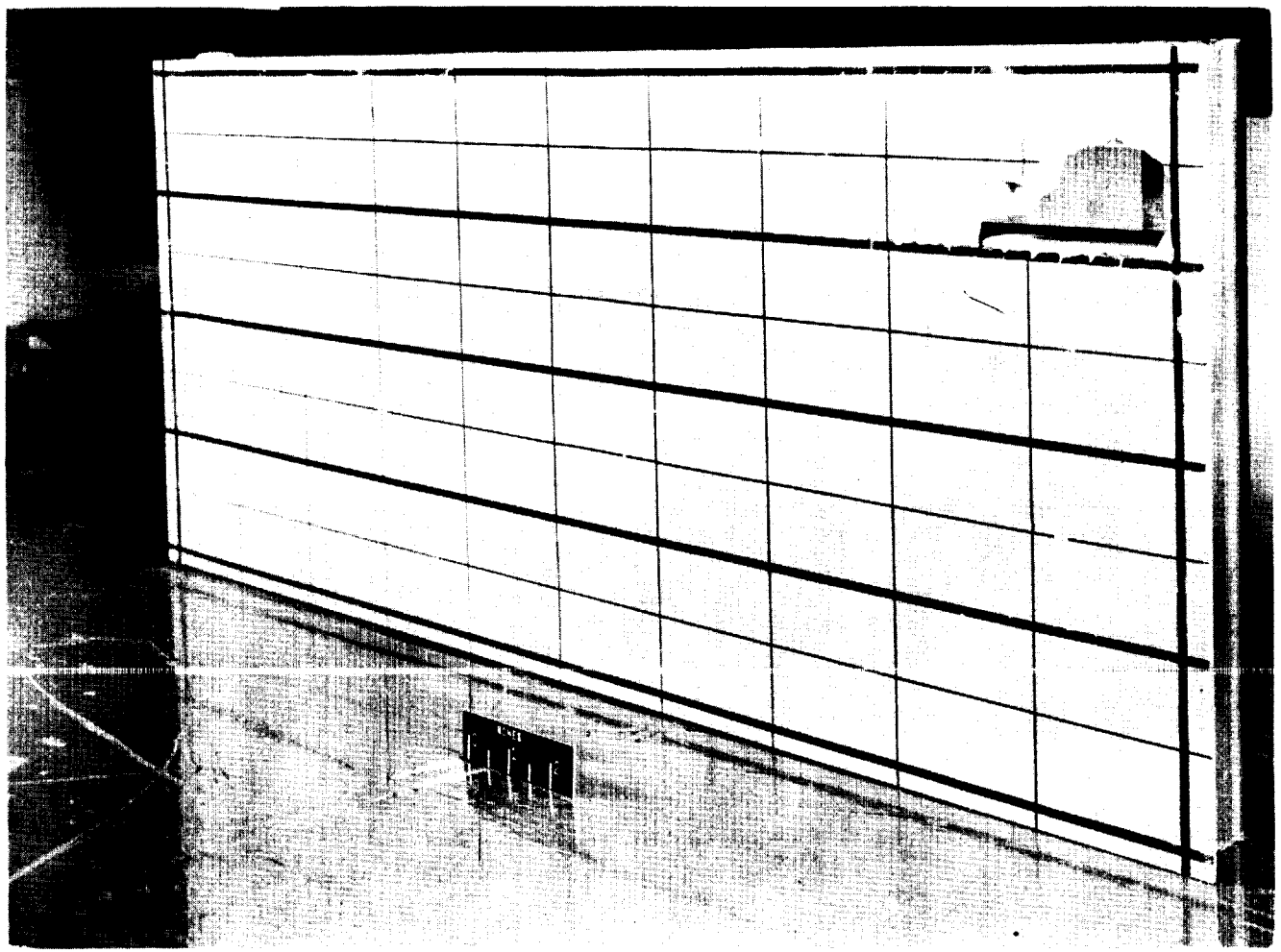

L-60-775.1

Figure 10.- Damage to panel (downstream end) with 0.025-inch-thick aluminum alloy skin after 17.5 seconds of flutter (test 1).

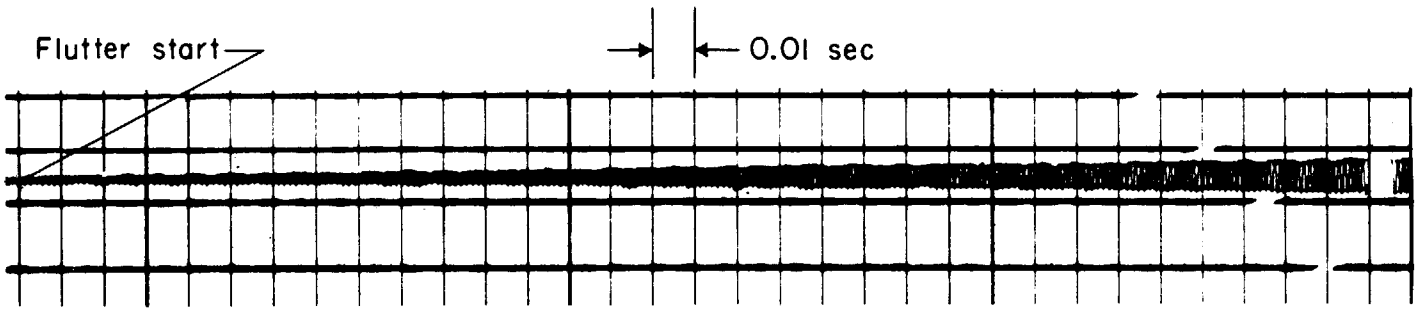

(a) Start of flutter under constant dynamic pressure (panel flat).

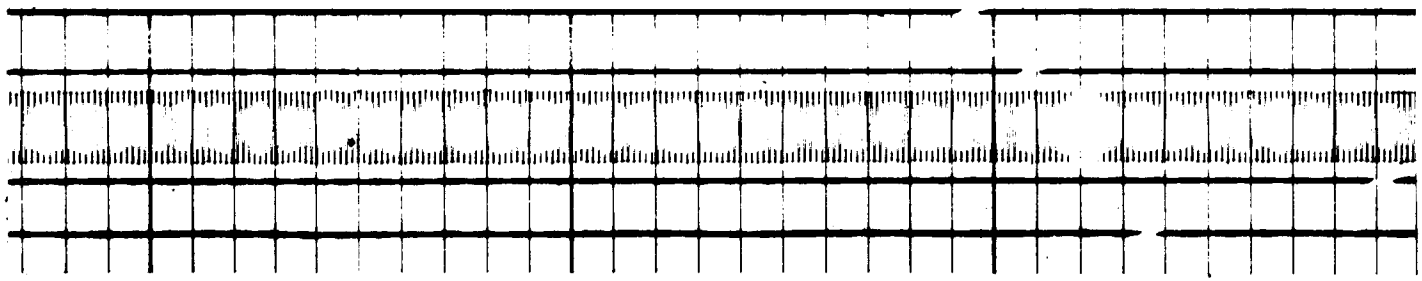

(b) Constant-amplitude flutter.

Figure 11.- Sample deflectometer records.

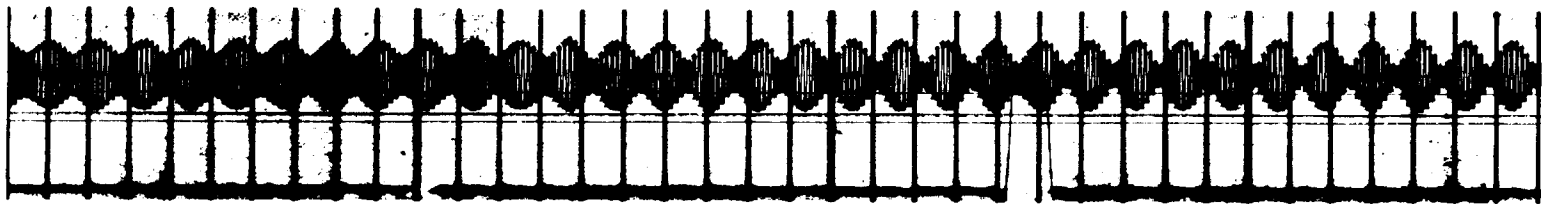

(c) Variable amplitude flutter similar to beating.

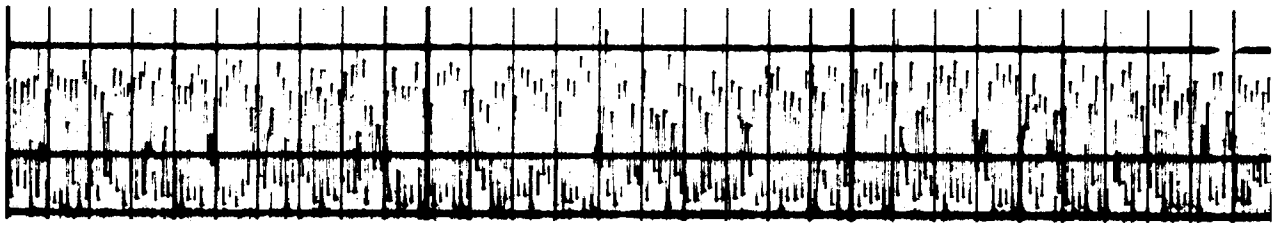

(d) Irregular amplitude flutter.

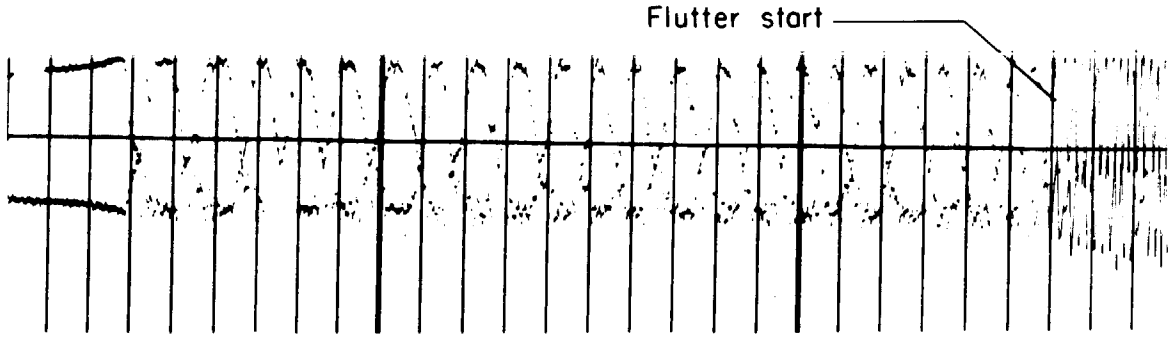

(e) Start of flutter under increasing dynamic pressure (panel buckled). (Two traces are shown.)

Figure 11.- Continued.

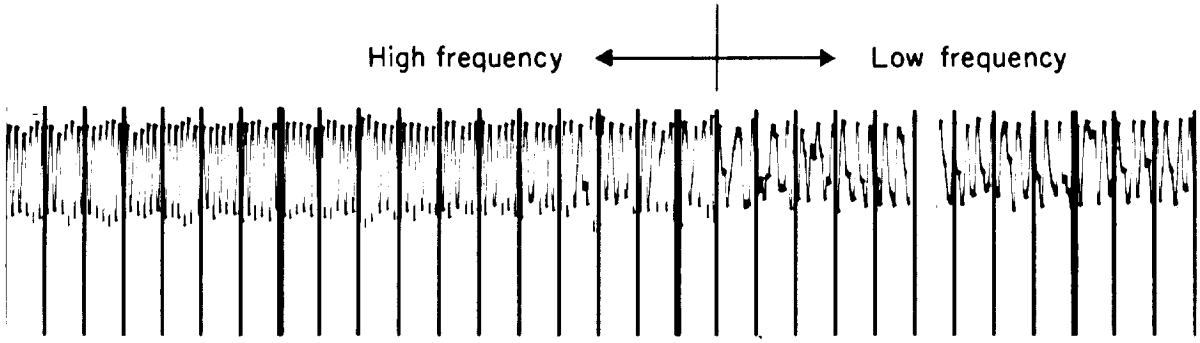

Abrupt change in frequency

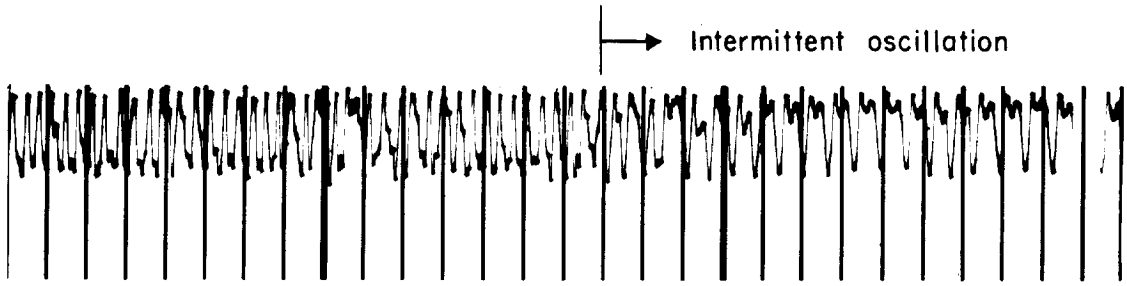

Transition to intermittent oscillation of buckles

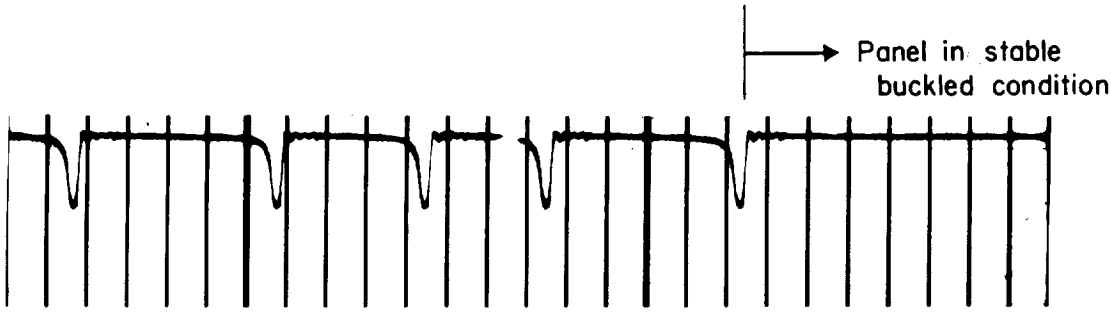

Intermittent oscillation of buckles stops

(f) Cessation of flutter under constant dynamic pressure (panel buckled).

Figure 11.- Concluded.

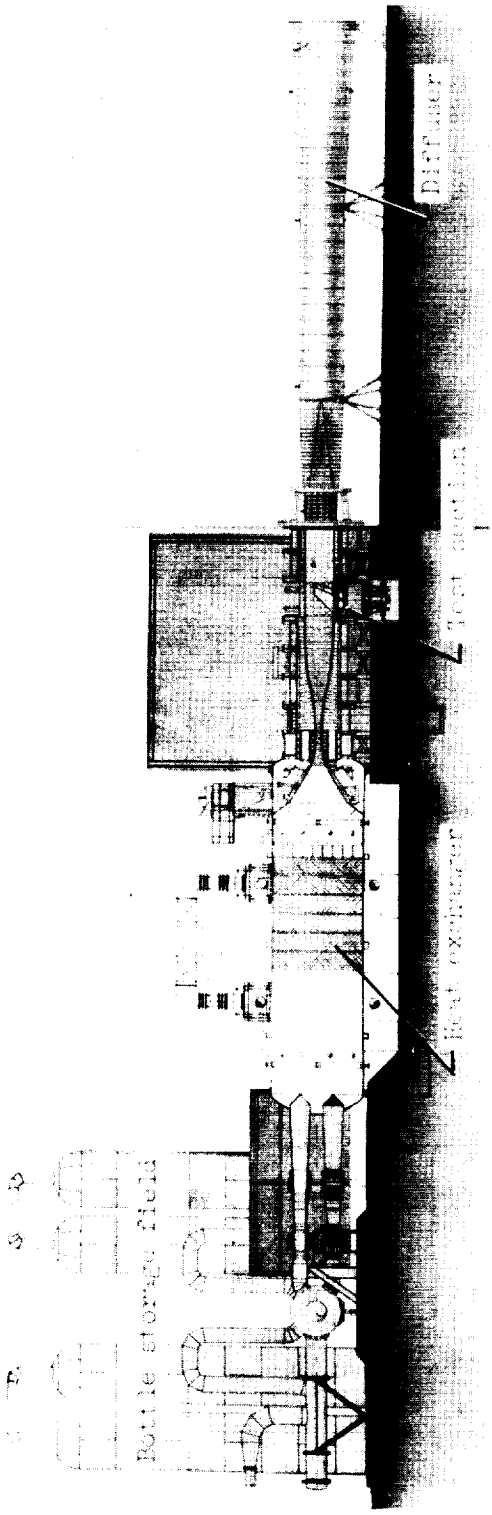

L-60-7256.1

Figure 12.- Cross section of 9- by 6-foot thermal structures tunnel.

L-1265